ISSN 0735-2727, Radioelectronics and Communications Systems, 2024, Vol. 67, No. 5, pp. 238–248. © Allerton Press, Inc., 2024.
Ukrainian Text © The Author(s), 2024, published in Izvestiya Vysshikh Uchebnykh Zavedenii, Radioelektronika, 2024, Vol. 67, No. 5, pp. 268–279.

Formation of Quadrature Components with Error Estimation for I/Q-Demodulators

Vadym Slyusar[a, *] (ORCID: 0000-0002-2912-3149)
and Nataliia Bihun[a, **] (ORCID: 0000-0003-3327-5521)

[a]*Central Scientific Research Institute of Armament and Military Equipment of the Armed Forces of Ukraine, Kyiv, Ukraine*
**e-mail: swadim@ukr.net*
***e-mail: bigun0714@ukr.net*

Received February 8, 2024; revised April 30, 2024; accepted May 7, 2024

Abstract—The paper investigates the influence of the choice of weighting coefficients on the formation of quadrature components in I/Q demodulators. It proposes methods to improve the accuracy of I/Q demodulation and minimize quadrature errors. Different configurations of 8- and 10-sample I/Q demodulators with open sets of weighting coefficients are considered. Using simulation, it has been shown that certain sets of coefficients can significantly improve the amplitude-frequency characteristics, achieving a bandwidth narrowing of 1.5–1.7 times and better suppression of out-of-band interference. The synthesis of new sets of coefficients for 10-sample I/Q demodulators is also investigated, which leads to improved amplitude-frequency characteristics and reduced phase errors. The equivalence between combinations of two-stage demodulators and their single-stage counterparts is established, providing potential computational efficiency advantages. The proposed 13- and 15-sample equivalent filters demonstrate a high frequency filtering efficiency and zero orthogonalization error, making them a promising alternative to 16-sample demodulators. The obtained results emphasize the importance of choosing weighting coefficients to optimize the performance of I/Q demodulators and contribute to developing more accurate and efficient digital communication systems with increased noise immunity.

Keywords: Quadrature components, I/Q demodulation, phase errors, amplitude-frequency response (AFR), phase-frequency response (PFR), signal processing, telecommunications

DOI: 10.3103/S0735272724070021

1. INTRODUCTION

I/Q demodulation is the primary process in digital information systems that extracts information from modulated signals in various applications, from wireless systems and satellite communications to radar complexes [1]. The accuracy of demodulation directly affects the reliability of reception and minimization of bit errors, thereby maintaining the integrity and a high quality of data transmission [2].

However, the operation of I/Q demodulators can be complicated by the so-called quadrature errors, which arise due to the mismatch in amplitude and phase between the in-phase (I) and quadrature (Q) channels. Such errors can significantly degrade the demodulation performance, causing signal distortion and increasing the probability of bit errors [3]. Although there are various methods for reducing quadrature errors, such as blind estimation algorithms and machine learning-based approaches, they often require complex computations or have limitations in specific scenarios [4].

Unlike the approach in paper [5], which focuses on the transition to single-stage schemes, in this paper, optimizing weighting factors in multistage I/Q demodulators allows us to achieve the performance improvement without changing the structure. Therefore, there is a need for further research on optimizing I/Q demodulation processes and minimizing quadrature errors [6], paving the way to more efficient and reliable communication systems [7].

In paper [8], the authors proposed algorithms for the blind estimation of the I/Q imbalance of I/Q receivers with direct down-conversion, solving the critical problem of I/Q imbalance caused by the amplitude and phase mismatch between the receiver channels. The proposed lower complexity algorithm [8] is based on the joint use of first- and second-order statistics that significantly simplifies the procedure for estimating the I/Q imbalance parameters and contributes to achieving ideal values of the bit error rate in the digital domain.

The authors of the paper [9] focused on compensating the I/Q imbalance in terahertz wireless systems using machine learning methods. They developed the architecture for transmitters and receivers that eliminates the impact of the imbalance without the need for direct estimation of the coefficients, demonstrating the high potential of machine learning in solving the hardware problems.

The studies in paper [10] are devoted to analyzing the impact of I/Q imbalance on the localization accuracy in millimeter-wave 5G systems. The paper shows that the amplitude-phase mismatch in the transmitter and receiver can significantly distort the position and orientation estimates, emphasizing the need for effective compensation methods. In paper [11], the authors consider the receiver circuits considering the I/Q imbalance for high-frequency multi-cell networks with massive MIMO and show that the failure to consider this factor leads to significant performance losses. At the same time, the proposed approach eliminates both the multi-user interference and the I/Q imbalance, emphasizing the need for a comprehensive consideration of this factor in massive MIMO systems.

In paper [12], a technique was developed for calibrating the mismatch errors in amplitude-digital converters based on backward propagation, which is suitable for digital receivers. This method not only reduces the jitter errors in amplitude-digital converter [13], but also allows for joint compensation of other disturbances, such as I and Q mismatches, which once again illustrates the multifaceted approach required to solve the problem of quadrature errors in modern communication systems.

Despite various methods and algorithms, the problem of optimizing I/Q demodulation processes and minimizing the quadrature errors remains open. This paper considers an approach that analyzes the influence of weighting coefficients on the formation of quadrature components of I/Q demodulators. The primary focus is on the extent to which the choice of optimal coefficients can improve demodulators' amplitude-frequency and phase-frequency responses, thus contributing to the construction of more accurate and reliable communication systems. The results are expected to positively impact the further development of high-performance I/Q demodulators and improve digital communication technologies.

2. SIMULATION WITH DIFFERENT WEIGHTING COEFFICIENTS IN SECOND STAGE OF I/Q DEMODULATORS

With the advent of digital communication, more sophisticated signal processing techniques have emerged to protect the quality and integrity of the transmitted information. This paper presents the methodology planned to improve the accuracy of the I/Q demodulation of signals using analysis and optimization techniques. A new method for reducing common phase errors in signal I/Q demodulation is investigated. Such solutions provide a high level of digital communication, which arises from a combination of theoretical modeling and real data analysis.

2.1. Nonidentity of Weighting Coefficients

To study the influence of phase errors on the result of forming the quadrature signal components in an 8-sample I/Q demodulator, we simulated I/Q demodulators of the same order that differed in weighting coefficients in the quadrature subchannels of the second stage of quadrature demodulation (Fig. 1).

In this case, signal processing in the first demodulation stage was simulated in the Mathcad package according to the circuit of 8-sample demodulator using the following expressions:

$$U^{s} = 1U_{0}^{c} - 11U_{2}^{c} + 15U_{4}^{c} - 5U_{6}^{c}, \quad (1)$$

$$U^{c} = 5U_{1}^{c} - 15U_{3}^{c} + 11U_{5}^{c} - 1U_{7}^{c}, \quad (2)$$

where superscrips "*s*" and "*c*" correspond to the sin and cos components, and second stage of I/Q demodulation was formed as two subchannels of 8-sample demodulators with different weighting coefficients.

In paper [15], an 8-sample I/Q demodulator with coefficients {1; 11; 15; 5} was considered, proving that such an 8-sample variant was not the only possible one. In addition, it is not the best way to minimize the amplitude-frequency characteristic (AFR) bandwidth.

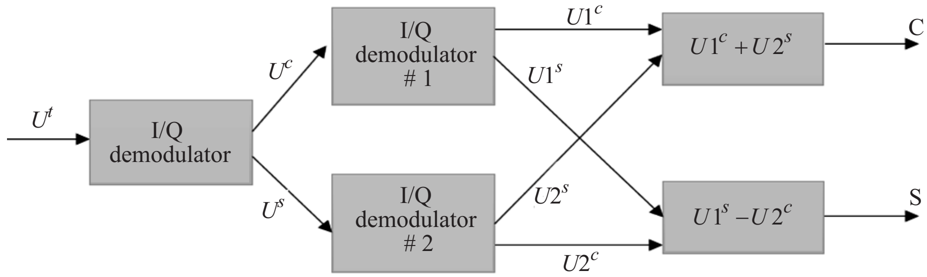

Fig. 1. Nonidentical I/Q demodulators (#1 and #2) in second stage [14].

Narrower bandwidths of the amplitude frequency response can be obtained by using the weighting factors {1; 5; 7; 3} or {2; 7; 10; 5}, which are a solution of indeterminate system of equations formed from the set of inequalities used in the calculation of the known weighting factors {1; 11; 15; 5}. Given this, when forming a mathematical model of quadrature responses of two subchannels of the second demodulation stage, coefficients {1; 11; 15; 5} and {1; 5; 7; 3} were chosen, as described by the following equations:

$$A1U1_0^s = 1U_0^c - 11U_2^c + 15U_4^c - 5U_6^c, \tag{3}$$

$$A1U1_0^c = 5U_1^c - 15U_3^c + 11U_5^c - 1U_7^c, \tag{4}$$

$$A2U2_0^s = 1U_0^s - 5U_2^s + 7U_4^s - 3U_6^s, \tag{5}$$

$$A2U2_0^c = 3U_1^s - 7U_3^s + 5U_5^s - 1U_7^s, \tag{6}$$

where $A1U$ and $A2U$ are the intermediate quadrature responses of two subchannels of the second stage of I/Q demodulation, formed by convolution of the weighting coefficients with the input signal U. They are used to calculate the final output responses $U2^c$ and $U2^s$.

Next, the cross-quadrature processing of the responses was performed at the output of the second stage according to the following scheme:

$$U2_0^c = A1U_0^s + A2U_0^c, \tag{7}$$

$$U2_0^s = A1U_0^c - A2U_0^s. \tag{8}$$

The phase error between the in-phase ($U2^c$) and quadrature ($U2^s$) signal components is calculated for a pair of the adjacent 10th and 11th time samples of the demodulator. To accurately determine this error, the arctangent ratio of the difference between the phase components of the signal is used.

The following expression determines the phase error:

$$\Delta\varphi = \arctan\left[\frac{U2_{10}^s U2_{10}^c + U2_{11}^s U2_{11}^c - (U2_{10}^s U2_{11}^c + U2_{11}^s U2_{10}^c)\cos(2\pi\tau f_2)}{(U2_{10}^s U2_{11}^c - U2_{10}^c U2_{11}^s)\sin(2\pi\tau f_2)}\right], \tag{9}$$

where $U2^c$ and $U2^s$ are the in-phase and quadrature components of the signal for time samples, τ is the sampling period for a 1/4 period of the central frequency of the working band of the I/Q demodulator, and f_2 is the sampled frequency of the signal (conventional units).

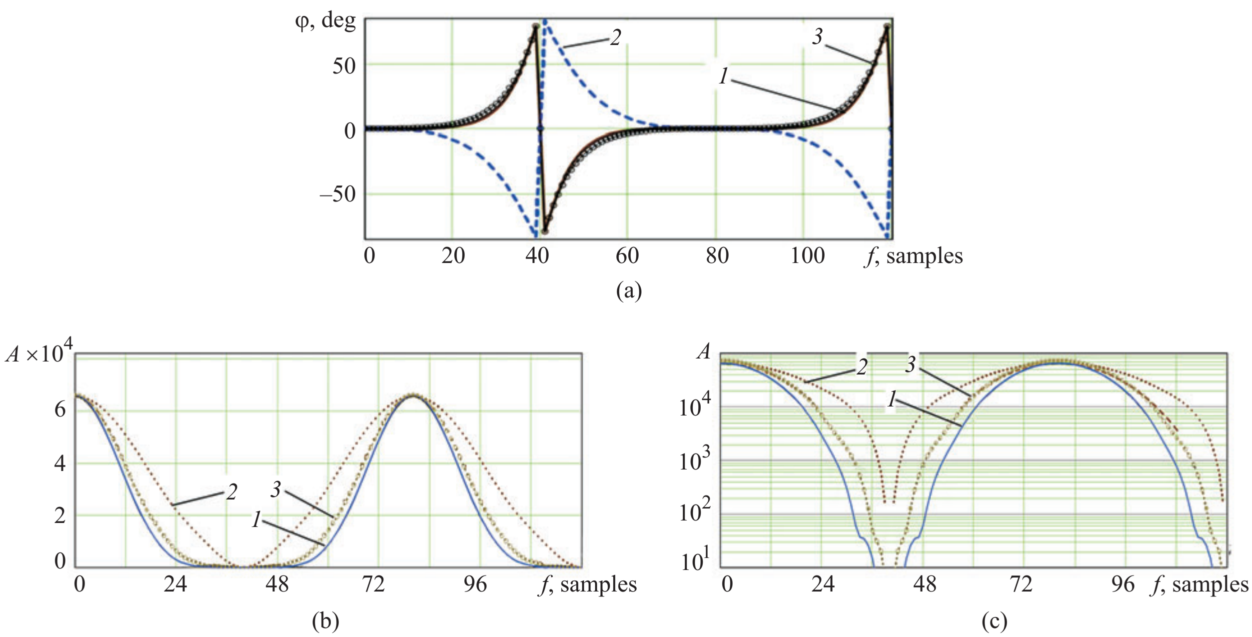

Fig. 2. PFR (a) and AFR in linear (b) and logarithmic scale (c) of 8-sample I/Q demodulators with coefficients {1; 11; 15; 5} (*1*), {1; 5; 7; 3} (*2*) in both channels, and 1st subchannel {1; 11; 15; 5} and 2nd subchannel {1; 5; 7; 3} (*3*).

The numerator of formula (9) consists of products of the quadrature and in-phase components of the signal, both of each time sample separately and crossed between neighboring samples. These products are corrected by the phase shift using the cosine factor $\cos(2f_2)$, which considers the frequency correction.

The denominator of expression (9) contains cross products corrected by the sine factor $\sin(2f_2)$, which corrects changes in signal amplitude between adjacent samples.

Formula (9) allows us to accurately calculate the phase error for the quadrature components of demodulator, considering both the phase change between samples and the effect of the frequency and sampling period on the discrete signal.

To analyze the amplitude frequency response (AFR) and phase-frequency response (PFR) of I/Q demodulator signals, a complex vector of the demodulator output data was first generated in Mathcad package, which includes the results for different frequency ranges. At the end of the analysis, the maximum value was searched among the elements of the vector of amplitudes of the I/Q demodulator responses.

Figure 2(a) shows the PFR plots corresponding to the processing with nonidentical subchannels of the second stage of the circuit (Fig. 1). Here, the sets of coefficients {2; 7; 10; 5}, {1; 5; 7; 3}, and {1; 11; 15; 5} in the first subchannel of the second stage correspond to curves *1*, *2* and *3*, respectively. At the same time, in the second subchannel of the I/Q demodulator, coefficients {1; 5; 7; 3} were used. Figure 2(b) shows their respective AFR in linear and logarithmic formats, where amplitude A is measured in ADC quanta.

2.2. Nonidentity of Sliding Windows

As a second variant of nonidentities of processing subchannels in the second stage of the I/Q demodulator, we consider a set of 8-sample "sliding" windows with coefficients {2; 7; 10; 5} and {1; 5; 7; 3}:

$$A1U1_0^s = 2U_0^c - 7U_2^c + 10U_4^c - 5U_6^c, \tag{10}$$

$$A1U1_0^c = 5U_1^c - 10U_3^c + 7U_5^c - 2U_7^c, \tag{11}$$

$$A2U2_0^s = 1U_0^s - 5U_2^s + 7U_4^s - 3U_6^s, \tag{12}$$

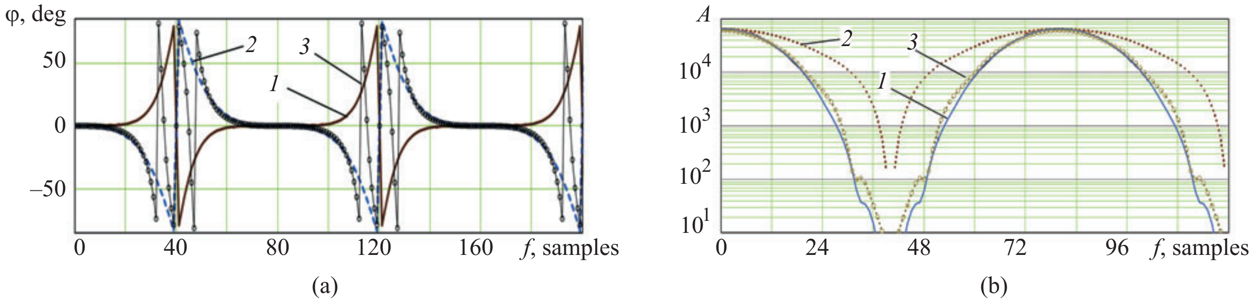

Fig. 3. PFR (a) and logarithmic AFR (b) of 8-sample I/Q demodulators with different sets of coefficients in subchannels of second stage {1; 11; 15; 5} (*1*), {1; 5; 7; 3} (*2*), and 1st subchannel {2; 7; 10; 5} and 2nd subchannel {1; 5; 7; 3} (*3*).

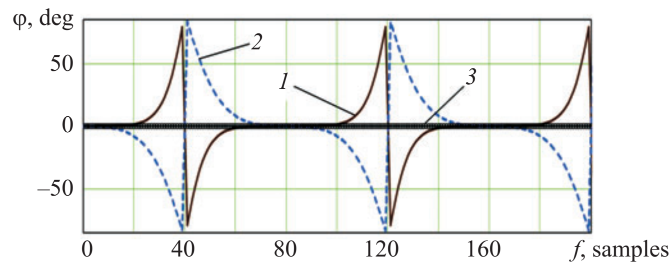

Fig. 4. PFR of 8-sample I/Q demodulators with identical coefficients in channels of second stage {1; 11; 15; 5} (*1*), {1; 5; 7; 3} (*2*), {1; 11; 15; 5} (*3*) in both subchannels.

$$A2U2_0^c = 3U_1^s - 7U_3^s + 5U_5^s - 1U_7^s. \tag{13}$$

Since the nonidentity of quadrature subchannels is more pronounced in this case, the phase errors appear more pronounced [Fig. 3(a)]. The corresponding variant of the AFR calculation using the logarithmic scale is illustrated in Fig. 3(b).

When the specified weighting coefficients in the subchannels of the second stage of I/Q demodulation are chosen identically, the phase errors are zero (Fig. 4). In this sense, the obtained two-stage I/Q demodulator repeats the properties of the digital Hilbert filter. Still, its advantage over the Hilbert filter is the absence of amplitude errors. This is corroborated by the shape of AFRs corresponding to nonidentical demodulators in quadrature subchannels. However, despite the nonidentity of subchannels, there are no distortions in AFRs.

The model of responses of the second stage of I/Q-demodulation used for identical subchannels is as follows:

$$A1U1_0^s = 1U_0^c - 11U_2^c + 15U_4^c - 5U_6^c, \tag{14}$$

$$A1U1_0^c = 5U_1^c - 15U_3^c + 11U_5^c - 1U_7^c, \tag{15}$$

$$A2U2_0^s = 1U_0^s - 11U_2^s + 15U_4^s - 5U_6^s, \tag{16}$$

$$A2U2_0^c = 5U_1^s - 15U_3^s + 11U_5^s - 1U_7^s. \tag{17}$$

3. SYNTHESIS AND ANALYSIS OF 13- AND 15-SAMPLE EQUIVALENT I/Q DEMODULATORS

The response of the 13-sample equivalent filter obtained by a series connection of 6-sample and 8-sample I/Q demodulators with coefficients {1; 4; 3} and {1; 5; 7; 3}, respectively, can be written as follows:

$$W^s = U_0^c - 18U_2^c + 63U_4^s - 92U_6^s + 63U_8^s - 18U_{10}^s + U_{12}^s, \tag{18}$$

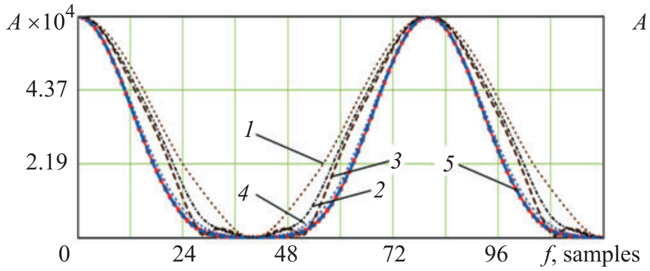

Fig. 5. Comparison of AFR of 8-sample (*1–3*, Fig. 2(a)), 16-sample (*4*) multistage version and equivalent single-stage (*5*) I/Q demodulators.

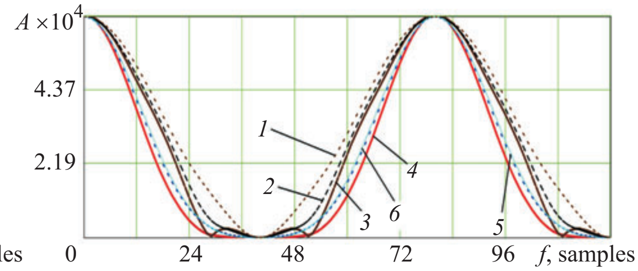

Fig. 6. Comparison of AFR of 8-sample (*1–3*, Fig. 2(a)), 13-sample (*4*, *5*), and 16-sample (*6*) I/Q demodulators.

$$W^c = 6U_1^c - 38U_3^c + 84U_5^s - 84U_7^s + 38U_9^c - 6U_{11}^s. \tag{19}$$

Figure 5 compares the amplitude frequency response (AFR) of I/Q demodulators of different structures and orders. Curves *1–3* correspond to the AFR of 8-sample I/Q demodulators with different sets of weighting coefficients [Fig. 2(a)]. They demonstrate the effect of the choice of coefficients on the AFR waveform and the bandwidth. Curve *4* shows the amplitude frequency response of the 16-sample demodulator synthesized using one independent variable with coefficients {1; 46; 265; 550; 627; 418; 131; 10}. This curve serves as a benchmark for comparing the performance of other demodulators. Curve *5* demonstrates the AFR of the 13-sample equivalent I/Q demodulator obtained by series connection of the 6-sample and 8-sample I/Q demodulators with coefficients {1; 4; 3} and {1; 5; 7; 3}, respectively, according to expressions (18) and (19).

The AFR analysis allows us to conclude that the 13-sample equivalent filter (curve *5*) demonstrates a high degree of coincidence with the AFR of the 16-sample I/Q demodulator (curve *4*). This means that the 13-sample I/Q demodulator can be an effective alternative to the 16-sample signal dequadrature filter, providing similar frequency-selective properties with less computational complexity and fewer samples.

An alternative 13-sample equivalent I/Q demodulator with the second stage coefficients {2; 7; 10; 5} (two stages with coefficients {1; 4; 3} and {2; 7; 10; 5}) is characterized by the following quadrature responses:

$$W^s = 2(U_0^c - 15U_2^c + 47U_4^s - 66U_6^s + 47U_8^s - 15U_{10}^s + U_{12}^s), \tag{20}$$

$$W^c = 11U_1^c - 59U_3^c + 122U_5^s - 122U_7^s + 59U_9^c - 11U_{11}^s. \tag{21}$$

This equivalent I/Q demodulator, as expected, has a better frequency selectivity than the procedure of (18) and (19). The mathematical model corresponding to the processing of (20) and (21) in operators of the Mathcad package can be written as follows:

MM16comopt(Uc) : = for r ∈ (0..Rline – 1)
| $Ucfrk\_s_{1,r} \leftarrow 2(Uc_{0,r} - 15Uc_{2,r} + 47Uc_{4,r} - 66Uc_{6,r} + 47Uc_{8,r} - 15Uc_{10,r} + Uc_{12,r})$
| $Ucfrk\_c_{1,r} \leftarrow (11Uc_{1,r} - 59Uc_{3,r} + 122Uc_{5,r} - 122Uc_{7,r} + 59Uc_{9,r} - 11Uc_{11,r})$
U2 ← i Ucfrk_s
CFRK ← Ucfrk_c + U2

Figure 6 shows the AFR plots of the 13-sample I/Q demodulator (20) and (21) (curve *4*), AFR of the 13-sample equivalent (18) and (19), and the 8-sample and 16-sample filters of I/Q demodulators. The curves in Fig. 8 correspond to the 8-sample I/Q demodulator with coefficients {1; 11; 15; 5} obtained with one independent variable (curve *1*); 8-sample demodulator with coefficients {1; 5; 7; 3} obtained with two independent variables (curve *2*), and 8-sample demodulator with coefficients {2; 7; 10; 5} also obtained with two independent variables (curve *3*). Curve *4* shows the 13-sample equivalent I/Q demodulator constructed by using coefficients {1; 4; 3} and {2; 7; 10; 5}, curve *5* represents another 13-sample equivalent demodulator with coefficients {1; 4; 3} and {1; 11; 15; 5}, and curve *6* corresponds to the 16-sample I/Q

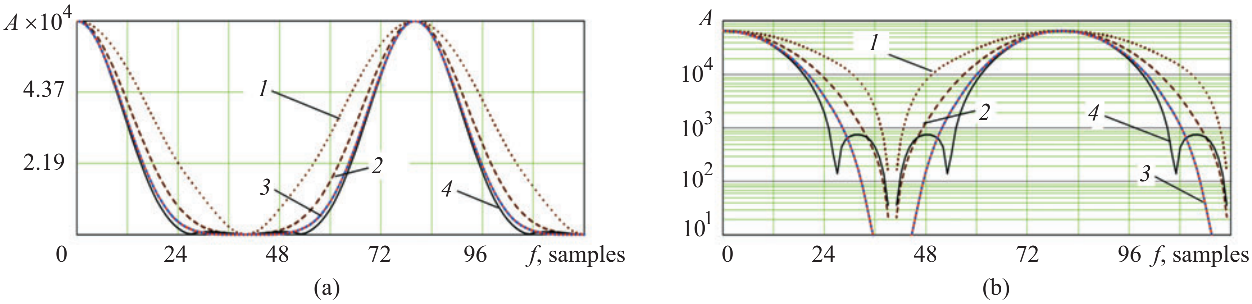

Fig. 7. Comparison of AFR (a) and logarithmic AFR (b) of 8-sample with coefficients {1; 11; 15; 5} (*1*) and {2; 7; 10; 5} (*2*), 15-sample (*3*), and 16-sample (*4*) I/Q demodulators.

demodulator with coefficients {1; 46; 265; 550; 627; 418; 131; 10} obtained with a single independent variable.

Figure 6 shows the advantages of using 13-sample equivalent I/Q demodulators compared to the 8-sample I/Q demodulators and 16-sample I/Q demodulator. Both versions of the 13-sample I/Q demodulators shown in Fig. 6 demonstrate a significantly narrower bandwidth and better frequency selectivity than the 8-sample I/Q demodulators.

In particular, the 13-sample I/Q demodulator with coefficients {1; 4; 3} and {2; 7; 10; 5} has the best properties of frequency selectivity among all the presented variants, including the 16-sample I/Q demodulator. This indicates the possibility of achieving a high filtering efficiency and I/Q-demodulation accuracy with fewer samples and reduced computational costs, which is important for practical applications. Thus, Fig. 6 confirms the results of the study and proves good prospects of using 13-sample equivalent filters to optimize I/Q demodulation.

Similarly, the response of the 15-sample equivalent I/Q demodulator obtained by series connection of two identical 8-sample stages with coefficients {1; 5; 7; 3} can be written in the form:

$$W^s = U_0^c - 19U_2^c + 81U_4^s - 155U_6^s + 155U_8^s - 81U_{10}^s + 19U_{12}^s - U_{14}^s, \tag{22}$$

$$W^c = 6U_1^c - 44U_3^c + 122U_5^s - 168U_7^s + 122U_9^c - 44U_{11}^s + 6U_{13}^s. \tag{23}$$

The corresponding model for forming the response of the 15-sample equivalent I/Q demodulator (22) and (23) in the Mathcad package is as follows:

VALEN(Uc) : = for r ∈ (0..Rline – 1)

| Ucfk_c_1, r ← $Uc_{0,r} - 19Uc_{2,r} + 81Uc_{4,r} - 155Uc_{6,r} + 155Uc_{8,r} - 81Uc_{10,r} + 19Uc_{12,r} - 1Uc_{14,r}$

| Ucfk_s_1, r ← $- 6Uc_{1,r} - 44Uc_{3,r} + 122Uc_{5,r} - 168Uc_{7,r} + 122Uc_{9,r} - 44Uc_{11,r} + 6Uc_{13,r}$

U2 ← i Ucfrk_s

CFRK ← Ucfrk_c + U2

The model employs the rearrangement of responses of the sine and cosine components that does not affect the shape of the AFR (Fig. 7). The following designations are used in Fig. 7: 8-sample I/Q demodulator with coefficients {1; 11; 15; 5} (curve *1*), 8-sample I/Q demodulator with coefficients {2; 7; 10; 5} (curve *2*), 15-sample equivalent I/Q demodulator with coefficients {1; 5; 7; 3} and {2; 10; 7; 5} (curve *3*), and 16-sample I/Q demodulator with coefficients obtained by using one independent variable {1; 46; 265; 550; 627; 418; 131; 10} (curve *4*).

The AFR analysis in Fig. 7 allows us to conclude that the 15-sample equivalent I/Q demodulator (curve *3*) demonstrates frequency-selective properties close to those of the 16-sample I/Q demodulator (curve *4*). This means that the 15-sample I/Q demodulator can be an effective alternative to the 16-sample I/Q demodulator, providing a similar performance with smaller samples and reduced computational cost. In addition, the 15-sample I/Q demodulator has a much narrower bandwidth and better out-of-band noise suppression than the 8-sample I/Q demodulators.

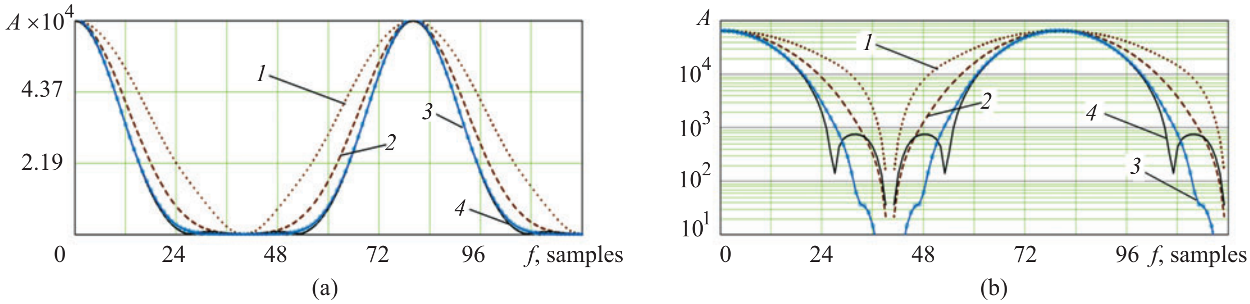

Fig. 8. Comparison of AFR (a) and logarithmic AFR (b) of 15-sample I/Q demodulator (24), (25) (*3*) in comparison with 8-sample with coefficients {1; 5; 7; 3} (*1*) and {2; 10; 7; 5} (*2*) and 16-sample (*4*) filters.

It should be noted that several different combinations of weighting coefficients are possible when forming the response of the 15-sample equivalent I/Q demodulator obtained by series connection of two 8-sample stages. In order not to overload the text with illustrative material, the results of calculating the amplitude frequency responses (AFR) of demodulators will be presented below only for the combination of weights {1; 5; 7; 3} in the first and {2; 10; 7; 5} in the second stage, and for the case of using the same weighting factors {2; 10; 7; 5} in both stages.

Thus, the response of the two stages of I/Q demodulators with coefficients {1; 5; 7; 3} and {2; 10; 7; 5} is determined by the following expressions:

$$W^s = 2U_0^c - 32U_2^c + 124U_4^s - 226U_6^s + 226U_8^s - 124U_{10}^s + 32U_{12}^s - 2U_{14}^s, \tag{24}$$

$$W^c = 11U_1^c - 70U_3^c + 181U_5^s - 244U_7^s + 181U_9^c - 70U_{11}^s + 11U_{13}^s. \tag{25}$$

Unlike previous cases where the coefficients were calculated using a single independent variable, this calculation uses two independent variables to increase the accuracy of the filter synthesis. The corresponding AFR are shown in Fig. 8, where the following notations are used: 8-sample filter with coefficients {1; 11; 15; 5} obtained in terms of one independent variable (curve *1*), 8-sample I/Q demodulator with coefficients {1; 5; 7; 3} obtained in terms of 2 independent variables (curve *2*), 15-sample equivalent I/Q demodulator (24) and (25) (curve *3*), and 16-sample I/Q demodulator with coefficients obtained in terms of two independent variables {1; 46; 265; 550; 627; 418; 131; 10} (curve *4*).

In the case of using two stages with identical coefficients {2; 10; 7; 5}, the relationships for the output quadrature signal of I/Q demodulator are as follows:

$$W^s = 4U_0^c - 53U_2^c + 189U_4^s - 330U_6^s + 330U_8^s - 189U_{10}^s + 53U_{12}^s - 4U_{14}^s, \tag{26}$$

$$W^c = 20U_1^c - 110U_3^c + 268U_5^s - 356U_7^s + 268U_9^c - 110U_{11}^s + 20U_{13}^s. \tag{27}$$

With due regard for the high efficiency of frequency filtering of the algorithm (26) and (27), in what follows, we do not consider the cases of combining the set of coefficients of the 8-sample I/Q demodulator {1; 11; 15; 5} with one of the new sets of weighting factors that are inferior in terms of the bandwidth.

All the considered equivalent odd-order I/Q demodulators have zero orthogonalization error in the entire possible frequency band. To illustrate this effect, the 15-sample I/Q-demodulator described by expressions (24) and (25) was simulated in the Mathcad package as follows:

$MAUs_{k,r}$:= $2Uc_{k,r} - 32Uc_{k+2,r} + 124Uc_{k+4,r} - 226Uc_{k+6,r} + 226Uc_{k+8,r} - 124Uc_{k+10,r} + 32Uc_{k+12,r} - 2Uc_{k+14,r}$

$MAUc_{k,r}$:= $11Uc_{k+1,r} - 70Uc_{k+3,r} + 181Uc_{k+5,r} - 244Uc_{k+7,r} + 181Uc_{k+9,r} - 70Uc_{k+11,r} + 11Uc_{k+13,r}$

FZM_r := atan[$(MAUs_{10,r}*MAUc_{10,r} + MAUs_{11,r}*MAUc_{11,r} - (MAUs_{10,r}*MAUc_{11,r} + MAUs_{11,r}*MAUc_{10,r})*\cos(2\pi*\tau*f2))/(-MAUs_{11,r}* MAUc_{10,r} + MAUs_{10,r}*MAUc_{11,r})\sin(2\pi*\tau*f2))$

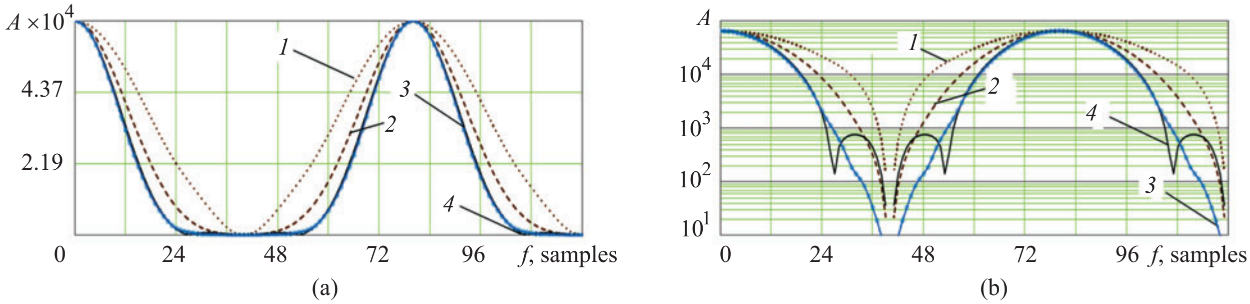

Fig. 9. Comparison of AFR (a) and logarithmic AFR (b) of 15-sample I/Q demodulator (26), (27) (*3*) in comparison with 8-sample with coefficients {1; 5; 7; 3} (*1*) and {2; 10; 7; 5} (*2*) and 16-sample (*4*) filters.

The simulation results are presented in Fig. 9 containing the following data: 8-sample I/Q demodulator with coefficients {1; 11; 15; 5} (curve *1*); 8-sample I/Q demodulator with coefficients {1; 5; 7; 3} (curve *2*), 15-sample equivalent I/Q demodulator (26), (27) (curve *3*), and 16-sample I/Q demodulator with coefficients {1; 46; 265; 550; 627; 418; 131; 10} obtained by using two independent variables (curve *4*).

The analysis of the AFR shown in Fig. 9 allows us to conclude that the algorithm (26) and (27) has frequency-selective properties that are practically similar to the 16-sample I/Q demodulator with coefficients {1; 46; 265; 550; 627; 418; 131; 10} synthesized by using two independent variables. Curve *3* indicates the complete identity of the AFRs of the 15-sample algorithm (26) and (27) and the corresponding two-stage procedure. The phase error versus frequency plot for such a 15-sample demodulator is shown in Fig. 10 (curve *2*).

4. CONCLUSIONS

The results of this study confirm that the optimal selection of weighting coefficients significantly affects the parameters of I/Q demodulators, in particular, the amplitude and phase-frequency characteristics, as well as the width of their passband [12]. The comparison of different configurations of I/Q demodulators has shown that the standard set of 8-sample coefficients {1; 11; 15; 5} of I/Q demodulators does not always optimal in terms of suppressing out-of-band components and minimizing phase errors. The proposed alternative sets of weighting coefficients allow narrowing the bandwidth by 1.5–1.7 times, which contributes to increasing frequency selectivity and effective suppression of out-of-band components without increasing computational complexity.

It is particularly noteworthy that when using the same coefficients in the quadrature subchannels of the second stage, it is possible to neutralize the phase error while maintaining the absence of amplitude distortion, i.e., to obtain a demodulator equivalent to the digital Hilbert filter, but without its inherent amplitude disadvantages [16].

The development and study of the 13- and 15-sample equivalent I/Q demodulators formed by cascading the previously analyzed blocks [17] have shown that their synthesis allows us to achieve the results comparable or better than those of the 16-sample I/Q demodulator, since the proposed solutions have similar or narrower bandwidths and a high degree of suppression of the out-of-band components.

In particular, the 13-sample structure formed using the 6- [20] and 8-sample demodulators with coefficients {1; 4; 3} and {2; 7; 10; 5} features the best frequency selectivity among all tested configurations. At the same time, the 15-sample demodulator, consisting of two 8-sample stages, retains the orthogonalization accuracy and close amplitude-frequency waveform inherent to the 16-sample solution, minimizing the need for computing resources, which improves system performance, significantly reducing computing costs.

Thus, the paper shows that the cascade connection of demodulators of different dimensions and the use of appropriate weighting coefficients can significantly improve the noise immunity and reduce phase errors during demodulation. In addition, the proposed configurations reduce the number of samples required for signal processing and maintain zero orthogonalization error over the entire operating frequency band.

The practical significance of the described approaches lies in the fact that they can be successfully implemented in high-speed communication systems of the fifth and sixth generations and in satellite and radar applications, where a narrower bandwidth and effective suppression of out-of-band components are particularly relevant. This opens up prospects for further improvement and adaptation of cascade I/Q

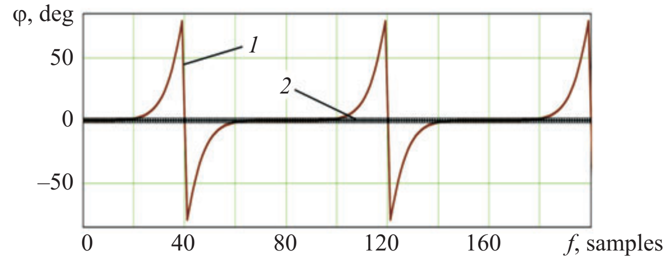

Fig. 10. PFR of 8-sample I/Q demodulators with coefficients {1; 11; 15; 5} (*1*) and 15-sample I/Q demodulator with identical coefficients {2; 7; 10; 5} (*2*).

demodulators by incorporating machine learning mechanisms or by varying the parameters in real time depending on the environmental conditions and modulation type [19].

ADDITIONAL INFORMATION

The initial version of this paper in Ukrainian is published in the journal *Izvestiya Vysshikh Uchebnykh Zavedenii. Radioelektronika*, ISSN 2307-6011 (Online), ISSN 0021-3470 (Print) on the link http://radio.kpi.ua/article/view/S0021347024070021 with https://doi.org/10.20535/S0021347024070021.

FUNDING

This work was supported by ongoing institutional funding. No additional grants to carry out or direct this particular research were obtained.

CONFLICT OF INTEREST

The authors declare that they have no conflicts of interest.

REFERENCES

1. N. T. Hieu, H.-G. Ryu, C.-X. Wang, and H.-H. Chen, "The impact of the I/Q mismatching errors on the BER performance of OFDM communication systems," in *2007 IEEE International Conference on Communications* (IEEE, 2007), pp. 5423–5427. https://doi.org/10.1109/ICC.2007.898.
2. F. Talebpour, A. Sali, R. Alirezaee, P. Varahram, and S. Alirezaee, "A novel robust technique to compensate I/Q imperfections in quadrature modulator using LMS algorithm," in *2021 International Conference on Electrical*, *Computer*, *Communications And Mechatronics Engineering* (*ICECCME*) (IEEE, Mauritius, 2021), pp. 1–9. https://doi.org/10.1109/ICECCME52200.2021.9590842.
3. H. Wu, B. Wu, X. Meng, Q. Bao, W. Wang, L. Ye, and X. Sun, "Enhanced imbalance-distortion mitigation and noise suppression in I~/~Q -based phase demodulation systems," *IEEE Sensors J.* **24**, No. 9, 14413 (2024). https://doi.org/10.1109/JSEN.2024.3374811.
4. W. Li, Y. Zhang, L.-K. Huang, J. Cosmas, C. Maple, and J. Xiong, "Self-IQ-demodulation based compensation scheme of frequency-dependent IQ imbalance for wideband direct-conversion transmitters," *IEEE Trans. Broadcast.* **61**, No. 4, 666 (2015). https://doi.org/10.1109/TBC.2015.2465138.
5. V. Slyusar and P. Serdiuk, "Synthesis method of procedure for odd-order I/Q demodulation based on replacing multistage with equivalent single-stage demodulation schemes," *Radioelectron. Commun. Syst.* **63**, No. 5, 273 (2020). https://doi.org/10.3103/S0735272720050064.
6. T. R. Clark, S. R. O'Connor, and M. L. Dennis, "A phase-modulation I/Q-demodulation microwave-to-digital photonic link," *IEEE Trans. Microw. Theory Tech.* **58**, No. 11, 3039 (2010). https://doi.org/10.1109/TMTT.2010.2076971.
7. J. J. de Witt, "Modelling, estimation and compensation of imbalances in quadrature transceivers," Dissertation presented for the degree of Doctor of Philosophy in the Faculty of Engineering at Stellenbosch University (2011).
8. P. Song, N. Zhang, H. Zhang, and F. Gong, "Blind estimation algorithms for I/Q imbalance in direct down-conversion receivers," in *2018 IEEE 88th Vehicular Technology Conference* (*VTC-Fall*) (IEEE, Chicago,

2018), pp. 1–5.
https://doi.org/10.1109/VTCFall.2018.8690669.

9. A.-A. A. Boulogeorgos and A. Alexiou, "Training terahertz wireless systems to battle I/Q imbalance," in *2023 International Balkan Conference On Communications And Networking* (*BalkanCom*) (IEEE, 2023), pp. 1–5. https://doi.org/10.1109/BalkanCom58402.2023.10167934.
10. F. Ghaseminajm, Z. Abu-Shaban, S. S. Ikki, H. Wymeersch, and C. R. Benson, "Localization error bounds for 5G mmWave systems under I/Q imbalance," *IEEE Trans. Veh. Technol.* **69**, No. 7, 7971 (2020). https://doi.org/10.1109/TVT.2020.2991377.
11. S. Zarei, W. H. Gerstacker, J. Aulin, and R. Schober, "I/Q imbalance aware widely-linear receiver for uplink multi-cell massive MIMO systems: design and sum rate analysis," *IEEE Trans. Wirel. Commun.* **15**, No. 5, 3393 (2016). https://doi.org/10.1109/TWC.2016.2520935.
12. F. Solis, B. T. Reyes, D. A. Morero, and M. R. Hueda, "Error-backpropagation-based background calibration of TI-ADC for adaptively equalized digital communication receivers," *IEEE Access* **10**, 103013 (2022). https://doi.org/10.1109/ACCESS.2022.3208092.
13. M. Bondarenko and V. I. Slyusar, "Influence of jitter in ADC on precision of direction-finding by digital antenna arrays," *Radioelectron. Commun. Syst.* **54**, No. 8, 436 (2011). https://doi.org/10.3103/S0735272711080061.
14. V. Slyusar and N. Bihun, "The method of increasing the immunity of data transmission in communication channels," in *2022 IEEE 9th International Conference on Problems of Infocommunications*, *Science and Technology* (*PIC S&T*) (IEEE, Kharkiv, 2022), pp. 301–305. https://doi.org/10.1109/PICST57299.2022.10238546.
15. V. Slyusar and N. Bihun, "Enhancing noise immunity in OFDM communication channels with two-stage strobing and I /Q demodulation," *Cybern. Syst. Anal.* **60**, No. 4, 667 (2024). https://doi.org/10.1007/s10559-024-00705-3.
16. C. Wu, Y. Wang, B. Nikolic, and C. Hull, "An interference-resilient wideband mixer-first receiver with LO leakage suppression and I/Q correlated orthogonal calibration," *IEEE Trans. Microw. Theory Tech.* **64**, No. 4, 1088 (2016). https://doi.org/10.1109/TMTT.2016.2532867.
17. V. Jain, F. Tzeng, L. Zhou, and P. Heydari, "A single-chip dual-band 22–29-GHz/77–81-GHz BiCMOS transceiver for automotive radars," *IEEE J. Solid-State Circuits* **44**, No. 12, 3469 (2009). https://doi.org/10.1109/JSSC.2009.2032583.
18. L. Li, D. Wang, X. Niu, Y. Chai, L. Chen, L. He, X. Wu, F. Zheng, T. Cui, and X. You, "mmWave communications for 5G: implementation challenges and advances," *Sci. China Inf. Sci.* **61**, No. 2, 021301 (2018). https://doi.org/10.1007/s11432-017-9262-8.
19. G. Di Rosa, "Digital optimization techniques for multi-band optical communication systems," Technische Universitaet Berlin: doctoral thesis (2023).
20. V. Slyusar and N. Bihun, "Forming the response of two-channel demodulators," in *2022 IEEE 2nd Ukrainian Microwave Week* (*UkrMW*) (IEEE, Ukraine, 2022), pp. 342–345. https://doi.org/10.1109/UkrMW58013.2022.10036993.

Publisher's Note. Allerton Press remains neutral with regard to jurisdictional claims in published maps and institutional affiliations.

AI tools may have been used in the translation or editing of this article.